Accepted Manuscript

Title: *Prosopis alba* exudate gum as novel excipient for fish oil encapsulation in polyelectrolyte bead system

Authors: Franco Emanuel Vasile, María Alicia Judis, María Florencia Mazzobre

Please cite this article as: Vasile, Franco Emanuel., Judis, María Alicia., & Mazzobre, María Florencia., Prosopis alba exudate gum as novel excipient for fish oil encapsulation in polyelectrolyte bead system.*Carbohydrate Polymers* http://dx.doi.org/10.1016/j.carbpol.2017.03.004

Prosopis alba exudate gum as novel excipient for fish oil encapsulation in polyelectrolyte bead system

Franco Emanuel Vasile[a,c,], María Alicia Judis[a], María Florencia Mazzobre[b,c]

[a] Laboratorio de Industrias Alimentarias II, Universidad Nacional del Chaco Austral, Comandante Fernández 755, Presidencia Roque Sáenz Peña (3700) Chaco, Argentina.

[b] Laboratorio de Conservación de Biomoléculas, Departamento de Industrias, Facultad de Ciencias Exactas y Naturales, Universidad de Buenos Aires, Ciudad Universitaria - Pabellón Industrias (1428) Buenos Aires, Argentina.

[c] Consejo Nacional de Investigaciones Científicas y Técnicas (CONICET). Argentina.

* Corresponding author. Tel.: +54 9 364 4420137 int. 114. Fax: +54 9 364 4420137. francovasile@uncaus.edu.ar. Comandante Fernández 755, Presidencia Roque Sáenz Peña (3700) Chaco, Argentina.

E-mail address: francovasile@uncaus.edu.ar (F. E. Vasile); majudis@uncaus.edu.ar (M. A. Judis); fmazzobre@di.fcen.uba.ar (M. F. Mazzobre)

Abbreviations

G: Prosopis alba exudate gum; *A*: Alginate; *Ch*: Chitosan; *FO*: Fish oil; *SO*: Surface Oil; *IO*: internal oil; *TO*: Total oil; *EE*: encapsulation efficiency; *EY*: encapsulation yield.

GRAPHICAL ABSTRACT
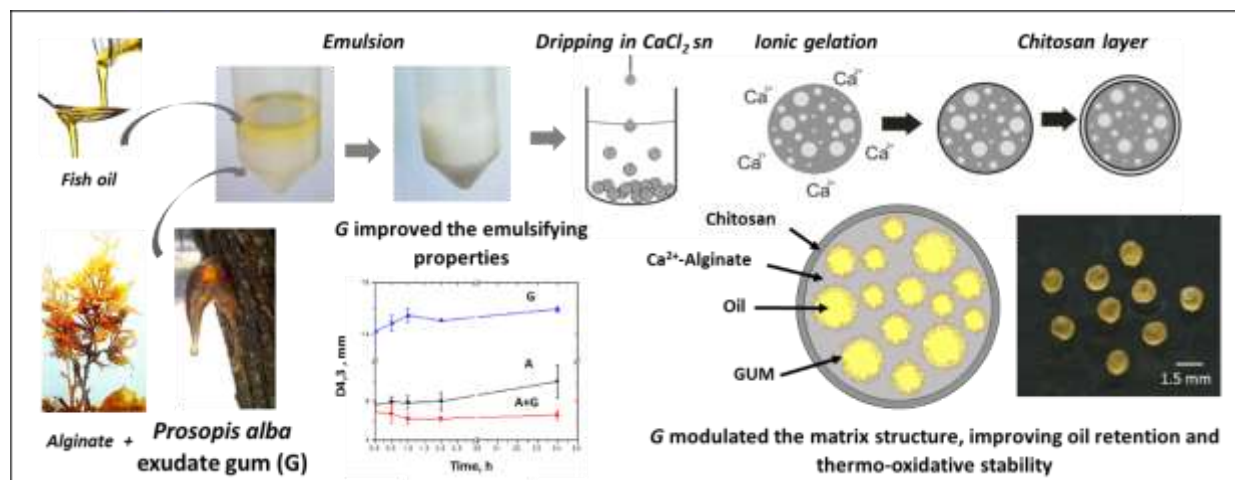
Highlights

- *Prosopis alba* exudate gum (G) was used as excipient in fish oil alginate beads.

- Polyelectrolyte interactions were study through sol-gel phase diagrams.

- Alginate-G suspensions are suitable for fish oil emulsification and beads generation.

- G introduction improves the encapsulation efficiency and yield after vacuum drying.

- G modulates the matrix structure, improving oil retention and oil thermo stability.

Abstract

In this work, a bottom-up approach based on the study of polyelectrolyte interactions was performed in order to evaluate the effect of *Prosopis alba* exudate gum as novel excipient for fish oil encapsulation in composed calcium-alginate-chitosan beads. Emulsion and beads properties such as oil distribution, encapsulation efficiency, yield, microstructure and thermo-oxidative protection were evaluated. Alginate and gum exert a synergistic effect on emulsion stability properties, which conducted to better oil distribution in the beads and higher encapsulation efficiencies (98%) and yield (89%). The positive effect of including the gum as wall material was observed in terms of a higher oil retention capacity of the alginate beads, improved oxidative thermal stability and better microstructural features. Present results are promising and allowed considering *P. alba* gum as a novel non-conventional polyelectrolyte for improving Ca-alginate beads microstructure and stability with the added benefit of taking advantage of an available resource currently untapped.

5

Chemical compounds studied in this article:

Sodium alginate (PubChem CID: 5102882); Chitosan (PubChem CID: 71853); Calcium chloride (PubChem CID: 5284359); hydrochloric acid (PubChem CID: 313); n-hexane (PubChem CID: 8058); ethanol (PubChem CID: 702); ethyl ether (PubChem CID: 3283).

1. Introduction

Alginate (A) is a natural polysaccharide derived from brown seaweeds (*Phaeophyceae*), and its basic structure consists of linear unbranched polymers containing α-(1→4)-linked D-mannuronic acid and β-(1→4)-linked L-guluronic acid residues arranged as linear homopolymeric and heteropolymeric blocks (Pawar & Edgar, 2012). Recognized gelation properties of A in presence of divalent cations has promoted its use for the encapsulation of several pharmaceuticals and nutrients (Lee & Mooney, 2012; Pongjanyakul & Puttipipatkhachorn, 2007). The entrapment of bioactives substances, is based on cross-linking of alginate uronic acids with cations as Ca^{2+}. The alginate matrix consisting of an open lattice structure forms porous beads (Bhattarai, Dhandapani, & Shrestha, 2011). Hence, the low retention capacity and high oxygen permeability could limit the use for protection and deliver of easily oxidizable compounds.

The encapsulation of many different oils for nutrition, therapeutics, and flavoring or aromas in alginate matrices has been reported (Abang, Chan, & Poncelet, 2012; Sun-Waterhouse, Zhou, Miskelly, Wibisono, & Wadhwa, 2011; Wang, Waterhouse, & Sun-Waterhouse, 2013). Particularly, for lipid encapsulation, alginate gel particles have been considered to be superior compared to those obtained by spray drying (Abang et al., 2012) since gelation can occur at mild conditions. However, these particles need a precise structuring of the encapsulating matrix to provide sufficient stability and protection to the core material. Physicochemical and delivery A-Ca^{2+} beads properties could be modified by incorporation of other substances to form composite gel systems (Córdoba, Deladino, & Martino, 2013; Wang et al., 2013; Wichchukit, Oztop, McCarthy, & McCarthy, 2013) and also by adsorption of the formed beads with a double or multiple coating (Bhattarai et al., 2011; Peniche, Howland, Carrillo, Zaldívar, & Argüelles-Monal, 2004). The mixture of alginate with other polymers have widely spread the functionality and usefulness of

alginate capsules in several applications (Pongjanyakul & Puttipipatkhachorn, 2007). Some water-soluble polymers were used to reinforce A-Ca^{2+} beads by allowing the formation of alginate hydrocolloids complexes. Surface-active hydrocolloids specially contribute with core material protection providing an integral part of the protective environment through its barrier properties (Drusch & Mannino, 2009). In almost all industrial techniques employed for microencapsulation of lipid substances, the first step is the preparation of an emulsion comprising the oil of interest and the encapsulation materials in aqueous form (Chan, 2011; Drusch & Mannino, 2009). Emulsifying constituent of the carrier matrix built a defined structure at the oil-water interface giving a solid multi-phase particle by gelation and subsequent water removal in the drying step (Drusch & Mannino, 2009). Thus, emulsions properties determines several properties of the encapsulates, mainly related to the retention and protection (Klaypradit & Huang, 2008). Therefore, one of the criteria for selecting encapsulation materials is based on its emulsifying activity (Chan, 2011).

Prosopis alba exudate gum (G) is the naturally occurring exudate obtained from branches and trunk of *P. alba* trees, widely spread in arid and semiarid regions of South America, especially at the north-east region of Argentine. It is a surface-active and water-soluble hydrocolloid with a considerable high protein fraction (13.81 ± 0,33 % db.), which shows emulsion properties similar and even superior of those of arabic gum (Vasile, Martinez, Ruiz-Henestrosa, Judis, & Mazzobre, 2016). However, this natural hydrocolloid resource is currently untapped. In a recent publication on functional properties of *P. alba,* we pointed out its usefulness as food additive or excipient in novel applications as encapsulating agent of polyunsaturated fatty acids rich oils (Vasile, Romero, Judis, & Mazzobre, 2016). This work showed that fatty acids quality and lipid health indices were widely preserved in beads containing the gum. From these studies we hypothesize that the introduction of G in A-Ca^{2+} beads may positively influence the structure and hence

improve the protection properties of the capsules containing highly oxidizable oils.

Therefore, a bottom-up approach based on hydrocolloids interactions with a precise

definition of the goals at each stage of the encapsulation process must be performed. In

the present work, composite beads of G and A, covered with chitosan and containing a

fish oil were prepared by ionic gelation method. The effect of *P. alba* exudate gum on

alginates suspensions was evaluated on fish oil emulsion properties and related with some

beads properties such as oil distribution, encapsulation efficiency, yield, microstructure

and thermo-oxidative protection.

2. Materials and methods

2.1. Materials

Prosopis alba exudate gum (G) (*Ara*: 0.67, *Gal*: 0.19, *Rha*: 0.01, *GlcUA*: 0.12; [η]: $1.77 \cdot 10^{-2}$ L·g^{-1}) was obtained by purification from exudates, manually collected from native and protected trees located in the central zone of the province of Chaco, in the northeast Argentina. The trees popularly known as *"Algarrobo blanco",* were botanically identified by the IBONE (Botanical Institute of the Northeast, Corrientes, Argentina). The samples included natural exudations (on the main trunk and branches) and also exudations produced by mechanical damages (due to agricultural practices and other types of wounds). The samples had a bitter taste, slightly sweet odor and variable colors (from clear amber to dark reddish brown). The collected exudates were prepared as previously described in Vasile et al. (2016). 20 g of collected gum nodules were dispersed in 100 ml of water, at 75 ºC under constant stirring for 1 h. The suspension was then clarified by filtration (Whatman No. 4, Uppsala Sweden) and the resultant solution was frozen at -40ºC and freeze-dried (Rificor, Model L-I-E300-CRT, Buenos Aires, Argentina). Commercial sodium alginate (A) was provided by Cargill (Buenos Aires, Argentina) (Algogel 6020, medium molecular weight 135 kDa, guluronic/mannuronic ratio 56/44). Chitosan (Ch) (medium molecular weight, 190–310 kDa with deacetylation degree of 75–85%) used in this study was purchased from Sigma–Aldrich (St Louis, MO, USA). Refined fish oil (FO) was cordially provided by GIHON (Mar del Plata, Argentina) and it was used as supplied, without previous purification. All other reactants (calcium chloride, hydrochloric acid, n-hexane, ethanol, petroleum ether and ethyl ether) were commercially available and used as received. Double distilled water was used in all experiments.

2.2. Methods

2.2.1. Phase diagrams for study of polyelectrolytes interactions

Phase diagrams were made to study the polyelectrolyte interactions and its effect on physical state of aqueous suspension prior to emulsification, and during gel formation by ionic gelation. Firstly, a binary phase diagram was made for A+G blends, varying A (0 – 3% w/v) and G (0 – 4% w/v) concentrations in aqueous suspensions at room temperature, according to a simple network approach (Correa, 2003; Mestdagh & Axelos, 1999). For that, 0, 0.1, 0.2, 0.3 and 0.4 g of G were introduced in 10 ml of aqueous dispersions containing 0, 0.1, 0.2 or 0.3 g of A in all blends combinations. Hydrocolloids dispersions were left standing overnight at 25 °C to complete the polymer hydration. After that, macroscopic physical sate of suspensions was visually characterized as SOL (flow when tube is inverted) or GEL (not flow when tube is inverted) states. Following the same approach, a ternary phase diagram was made introducing calcium (gelling agent) as third component. Three milliliters of double distilled water with 0, 0.015, 0.03, 0.045, 0.06, 0.075, and 0.09 g of $CaCl_2$ (0 - 3 % w/v) were introduced in 2 ml of A+G aqueous dispersions prepared with 0.02 g of A (1% w/v) and 0, 0.01, 0.02, 0.03, 0.04, 0.05 and 0.06 g of G (0 – 3 % w/v). Macroscopic physical sate of blends was immediately characterized after calcium introduction as *SOL* (flow) and *GEL* (not flow), the presence of syneresis (Syn), liquid outflow from gel, was also evaluated in the GEL systems. In both diagrams, the physical state of blends at each composition was registered in a bidimensional plot. The regions indicating the different phases were limited by lines separating the experimental points.

2.2.2. Effect of gum in the forming emulsion properties

2.2.2.1. Preparation of polyelectrolyte suspensions and fish oil emulsions

Aqueous suspensions of A (1% w/v), G (2% w/v) and A+G (1 % w/v of A and 2% w/v of G) in a final volume of 3 ml, were prepared. Individual or combined polyelectrolytes were dispersed in double distilled water and left standing overnight with gentle stirring to complete the biopolymers hydration at room temperature. Commercial fish oil was dispersed in aqueous hydrocolloid suspensions to obtain emulsions of 0.1 oil volume fraction. The pre-emulsion was performed for 2 min at medium speed with Ultra-turrax (T18 IKA, Staufen, Germany) and final emulsion was carried out at 20000 rpm for 3 min.

2.2.2.2.   Droplet size distribution

Droplet size distributions of emulsions were determined by static light scattering (SLS) using a Mastersizer 2000 device equipped with a Hydro 2000MU as dispersion unit (Malvern Instruments, Worcestershire, United Kingdom). The pump speed was settled at 1800 rpm. The refractive index (RI) of the disperse phase (fish oil, RI = 1.479) and its absorption parameter (0.001) were used.

Droplet size was reported as $D_{3,2}$ diameter (volume–surface mean diameter or Sauter diameter, Eq. (1)) and $D_{4,3}$ diameter (equivalent volume-mean diameter or De Broucker diameter, Eq. (2)).

$$D_{3,2} = \Sigma \ n_i \ d_i^3 \ / \ \Sigma \ n_i \ d_i^2 \tag{1}$$

$$D_{4,3} = \Sigma \ n_i \ d_i^4 \ / \ \Sigma \ n_i \ di^3 \tag{2}$$

where n_i is the number of particles of diameter d_i (Galazka, Dickinson, & Ledward, 1996; Leroux, Langendorff, Schick, Vaishnav, & Mazoyer, 2003).

$D_{4,3}$ provides a measure of the mean diameter of most of the droplets and is related to changes in droplet size involving destabilization processes so it is more sensitive to oil droplet aggregation (Galazka et al., 1996; Relkin & Sourdet, 2005) .

The droplet size values are reported as the average and standard deviation of duplicates, with ten readings made per duplicate. Readings were performed at 0, 0.5, 1, 2 and 24 h at room temperature, in order to evaluate the emulsion stability.

2.2.2.3.   ζ-potential measurements

ζ–potential measurements were performed in a dynamic laser light scattering (DLS) instrument (Zetasizer Nano–ZS, Malvern Instruments, Worcestershire, United Kingdom). The ζ–potential was evaluated from the electrophoretic mobility of the particles. The conversion of the measured electrophoretic mobility data into ζ–potential was done using Henry's equation Eq. (3) (Hunter, 2001):

$$U_e = 2\varepsilon\zeta f(Ka) / 3\eta \tag{3}$$

where U_e is the electrophoretic mobility, ε the dielectric constant, η the sample viscosity and $f(Ka)$ the Henry's function.

Emulsions were previously diluted 1:100 with water and put into disposable capillary cells (DTS1060, Malvern Instruments, Worcestershire, United Kingdom). The reported values are the average and standard deviation of duplicates, with five readings made per duplicate.

2.2.3.   Generation and characterization of polyelectrolyte bead systems

2.2.3.1.   Generation of encapsulates by ionic gelation

Ten grams of fish oil emulsions stabilized with A or A+G, were prepared as described above. Hydrogel beads were generated by emulsion dropping into a gelling bath. A peristaltic pump (Boading Longer Precision Pump Co, Model BT50-1J, Habei, China) fitted at 9 ± 0.1 rpm was used to drop the A or A+G emulsions into a 20 g/l $CaCl_2$ (Cicarelli, p.a.) aqueous solution. Cross-linking of alginate uronic acids with calcium cations is known to

occur through the "egg-box" model (Grant, Morris, Rees, Smith, & Thom, 1973). The tip of the needle (0.25 mm of inner diameter) was fixed at 6 cm above the surface of the crosslinking solution. The gelling bath was gently stirred with an orbital shaker to prevent the agglomeration of beads. After generation, the beads were hardened for 10 min in the $CaCl_2$ solution (Peniche et al., 2004) and then transferred into a 2% w/v chitosan solution (prepared in 0.1 M HCl) for others 10 min. Finally, beads were washed with $CaCl_2$ solution. The effect of vacuum and freeze drying methods were examined. Vacuum dried beads were obtained in an oven operating at a chamber pressure of 700 mbar (Fistreem International, Ltd., Loughborough, England) with dried silica gel as desiccant agent at 30 ºC during 24 h. Freeze dried beads were initially frozen at -40 °C and then freeze-dried (Rificor, Model L-I-E300-CRT, Buenos Aires, Argentina).

2.2.3.2. Accelerated oil extraction in beads systems

The accelerated solvent oil extraction was performed by successively removing the oil with n-hexane on recently prepared and vacuum or freeze-dried beads (500 mg). Extraction was performed on the same sample with aliquots of n-hexane increasing progressively the stirring time: 1, 3, 7, 13 and 22 min. Supernatant was separated by filtration and extracted oil was measured by weighing the oil after solvent evaporation until reaching constant weight. Extracted oil amounts were represented as accumulative mass of extracted oil regard to total oil for the entire extraction period and expressed as g surface oil/total oil in beads.

2.2.3.3. Thermo oxidative stability determination in DSC

Calorimetric analyses were carried out in oxidative conditions in order to analyze the onset of thermal oxidation. A differential scanning calorimetry (DSC) system (Mettler TA 4000, Columbus, Ohio, USA) with TC11 TA processor and GraphWare (TA72 thermal

analysis software) were used for thermal analysis. The instrument was calibrated for temperature, heat flow and enthalpy of melting using triply distilled water (m.p. 0.0 ºC, ΔH = 6.013 kJ mol−1), indium (m.p. 156.6 ºC, ΔH = 3.28 kJ mol−1), lead (m.p. 327.5 ºC, ΔH = 4.799 kJ mol−1) and zinc (m.p. 419.6 ºC, ΔH = 7.32 kJ mol−1). Analysis involved 40 µL aluminium pans (Mettler) containing 5–10 mg samples, hermetically sealed. An empty pan was used as reference. Each sample was heated at a rate of 10 ºC min^{-1} from 40 to 240 ºC (dynamic method). Onset temperature of oxidation was recorded as the temperature at which a change in slope of curve of heat flow versus temperature.

2.2.3.4. Distribution of oil in the beads

Oil distribution was evaluated in terms of surface (SO), internal (IO) and total oil (TO) fractions. SO was measured as the extracted oil after stirring in n-hexane without disruption of bead structure for during 60 s, assuming that this time was adequate in extracting the free oil from bead surface. Approximately 1 g of beads was shaken in a flask with 5 ml of n-hexane during 60 s. The supernatant was transferred to a previously weighted tube and the SO was determined by differences in weight after solvent evaporation under nitrogen atmosphere at room temperature. IO was determined by the acid hydrolysis method described in AOAC Official Method 14.019 (1984) with minor modifications in order to reduce the employed solvent volumes. Briefly, the beads without oil in the surface (obtained as described above), were mixed with 1 ml of ethanol, 5 ml of HCl (37%) and heated at 80ºC for 40 min with constant stirring. Then 10 ml of ethanol were added, and the sample was cooled at room temperature. After that, 12.5 ml of petroleum ether and 12.5 ml of ethyl ether were added and shaken vigorously for 60 s. Upper ethereal phase was separated and filtered. This procedure was repeated three times using 5 ml of the last solvent mixture. Oil in ethereal phase was quantified by solvent evaporation at 50 ºC and subsequent cooling. Finally, TO was calculated considering the

14

SO and IO determined for each system. All measurements were made in duplicate and expressed as g oil/ 100 g of beads. IO and TO measurements were combined to evaluate encapsulation efficiency according to Eq. (4):

$$EE = (IO / TO)*100\%$$ (4)

Additionally, IO was related with the initial mass of oil (MO) weighed to emulsion formulation in order to calculate encapsulation yield according to Eq. (5):

$$EY = (IO / MO)*100\%$$ (5)

Yield determination required a quantitative treatment of emulsions composition per individual encapsulation batch (10 g of emulsion). Oil mass used in each emulsion formulation was quantitatively related with the mass of obtained dehydrated beads and its average IO content.

2.2.3.5. Size distribution by image analysis

The percentage of size distribution of the beads was carried out by analyzing digital images (Deladino, Anbinder, Navarro, & Martino, 2008). Whit this purpose a digital camera (Canon PowerShot A70 3.2 Mpix, Canon Inc., Malaysia; with zoom fixed in 3.0X) installed on a binocular microscope (magnification 7x, Unitron MS, Unitron Inc., New York, USA) was employed. The pictures were analyzed with the free software ImageJ (http://rsb.info.nih.gov/ij/). Diameter was analyzed for at least 50 beads (dried systems). Measurements were grouped in continuous intervals (mm) and were depicted in a percentage frequency histogram.

2.2.3.6. Scanning electron microscopy

15

External morphology and internal structure of beads were observed with a scanning electron microscope (CARL ZEISS NTS, model SUPRA 40) equipped with field emission gun (FEG-SEM), detector InLes and a third generation column GEMINI®. To internal structure inspection, capsules were carefully cut in half with a scalpel. Free oil from intact and halves beads, was removed by shaking samples for 5 min with n-hexane prior to metalize samples. Images were collected at 100x and 2000x.

2.2.4. Statistical analysis

At least two replicate determinations were performed for each trial. A statistical analysis, when necessary, was carried out using ANOVA test and differences among compared samples were considered significant at $P>0.05$ (interval of confidence of 95%). All statistical analysis and data fitting were performed through GraphPad Version 4 (GraphPad, Software Inc., San Diego, CA, USA).

3. Results and discussion

3.1. Study of *P. alba* gum-alginate interactions by Sol-Gel phase diagrams

The physical state of aqueous dispersions containing encapsulating materials, determines their applicability as actives dispersant phase in ionic gelation processes. The formation of a gel, hinder the later stages of emulsification of the active compound and transport required for ionic gelation encapsulation, thus combined polyelectrolytes formulations would be limit to concentrations where suspension remains fluid (not gel). In this sense, the physical state of combined suspensions containing sodium alginate and a novel exudate gum (*Prosopis alba)* were firstly studied. In order to identify the concentrations at which suspensions of A and G are suitable for emulsifying the oil (which will be then encapsulated by ionic gelation), binary phase diagrams were constructed as shown in Figure 1A.

Figure 1. Binary phases diagram for alginate - gum (A), and ternary phases diagram for alginate (1 % w/v) - gum - CaCl$_2$ blends (B) at 25 °C. Theoretical phase line separates experimental points and define SOL (fluid), GEL (not fluid) and Syn (syneresis, liquid outflow from gel) at each composition.
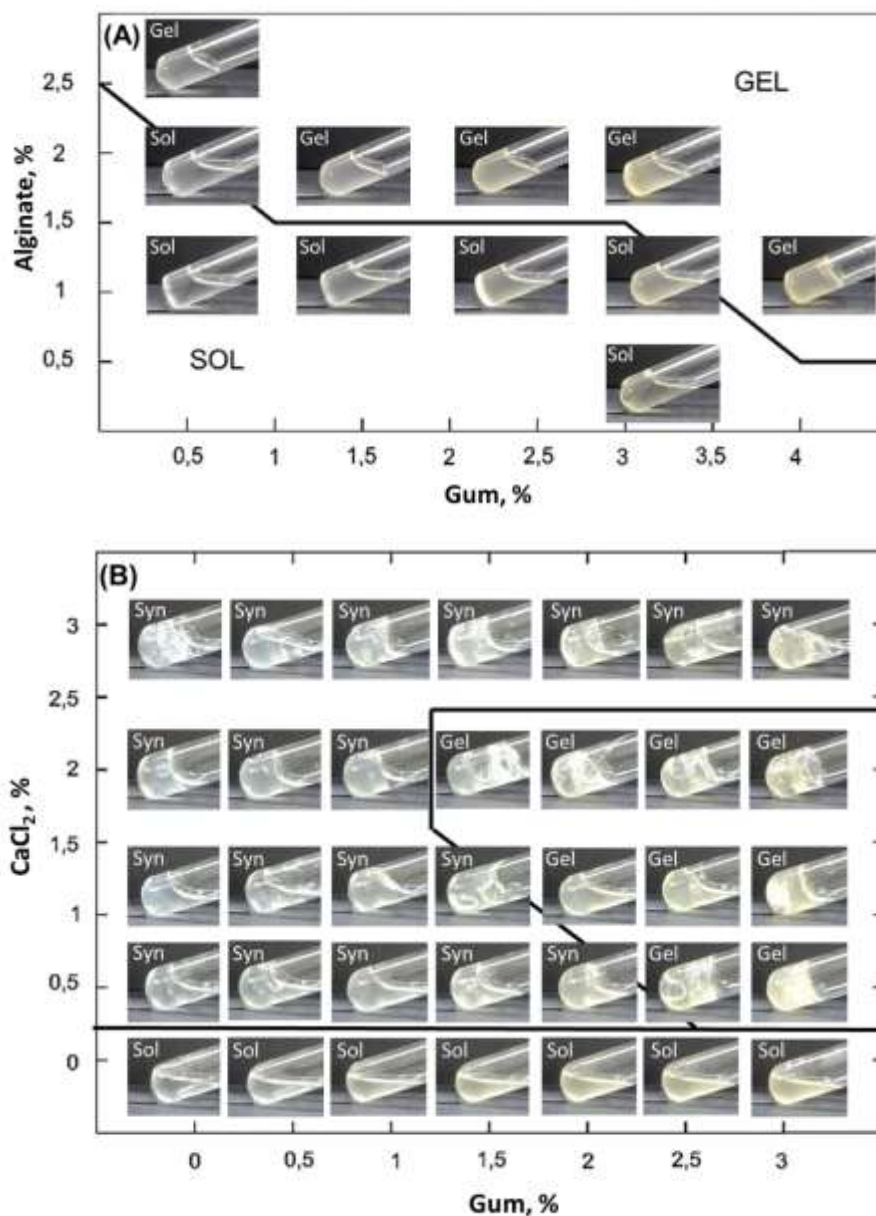
G+A mixtures did not show macroscopic phase separations at any of the concentrations studied, indicating good miscibility between polymers. Two distinct physical states (SOL, GEL) were observed and limited by a theoretical phase line (Figure 1A). Below the line, the systems were fluids (SOL phase), with homogeneous and translucent

aspect. At concentrations above the theoretical line, viscosity increased and a gel was formed. Increasing G fraction promoted gel formation and reduced the minimal concentration of A at which A+G suspensions remained fluid. Gelation of A+G blends was related with the introduction of Ca^{2+} naturally present in G ($4,61 \pm 0,02$ mg / g gum db.), which exerts a known viscosity increase of A suspensions even at low ion concentrations (BeMiller & Huber, 2007). Additionally, specific interactions between polyelectrolytes could contribute to gel structuring. According to Pongjanyakul et al. (2007) saccharide chains are able to form intermolecular associations by electrostatic interactions. In this sense, hydroxyl and carboxyl groups present in G (Vasile, Martinez, et al., 2016) could form intermolecular hydrogen bonds with A, increasing the viscosity of the composite dispersion. Additionally, positively charged amino groups from amino acids moieties in G, could interact with negatively charged carboxylic groups of A via electrostatic interactions promoting a similar effect. Individual interactions could have a synergistic influence on the consistency of composite dispersions. The analysis of the phase diagram (Figure 1A) allowed to conclude that the mixture G+A has a narrow range of concentrations (A 0.5 to 1% and G 0.5 to 3%) for which the mixture of hydrocolloids has an adequate fluidity to prepare emulsions containing the active of interest (fish oil) and for its further transport (via injection or dripping) in the capsules generation process.

Besides knowing the combinations of G and A suitable for generating the emulsion, in the encapsulation step is essential to establish the relative concentrations of A, G and $CaCl_2$ at which the system gels.

Although low concentrations of A support a greater proportion of G without occurring gelation (Figure 1A), it is known that concentrations of A lower than 1% w/v lead to the formation of weak and unstable gels during gelation in the presence of Ca^{2+} (Rehm, 2009). Furthermore, 1% w/v of A is the maximum concentration that allows evaluating different G proportions without spontaneous gelation (Figure 1A). Thus, an alginate concentration of

1% w/v was fixed to explore the influence of G and $CaCl_2$ proportions in the A-Ca^{2+} gel formation. With this purpose, a ternary phase diagram (Figure 1B) was built to determine the concentrations at which the formation of the gel occurs instantaneously, condition required for the generation of capsules by dripping.

The diagram shows the physical states of A+G blends immediately after the addition of calcium as third component. SOL and GEL states and the presence of syneresis were determined at different G and $CaCl_2$ concentration.

$CaCl_2$ concentrations equal or superior to 0.5 % w/v promoted the change of A fluid dispersions to gelled structures regardless of G concentration. However, at G concentrations lower than 2.5 % w/v the gels presented syneresis indicating that gelation was not completed, or that strong polymer-ion-polymer interactions promoted a reduction of the water holding capacity of the polymeric matrix (Rehm, 2009). Syneresis involves a partial liquid separation from a gelled matrix. When the gel is generated from an emulsion as in the present work, syneresis may result in the loss of the emulsified oil with the consequent undesired reduction of entrapment efficiency.

It was observed that higher concentration of G, lower concentrations of Ca^{2+} were necessary to obtain a gel without syneresis. G could act providing Ca^{2+} ions naturally present in its composition, and promoting thus the gelation. G also could act increasing the water holding capacity by its inherent hygroscopicity or well, by hindering the A-Ca^{2+} interactions. At $CaCl_2$ concentrations higher than 3 % w/v, syneresis was observed at any of the gum concentrations studied.

Any experimental point within the GEL region leads to spontaneous gel formation without syneresis. This conditions are highly desirable during beads formation by dripping method (Correa, 2003) since promote higher entrapment of core material. From binary and ternary phase diagrams analysis, the composition of hydrocolloids dispersant phase and gelling bath concentration could be properly defined. Particularly, an aqueous suspension

composed by 1% of A and 2% of G remains fluid for emulsion and dropping process and gels spontaneously at $CaCl_2$ concentration of 2%, giving a gel structure with adequate water holding capacity.

3.2. Emulsifying and stabilizing properties of the gum on alginate suspension

Most industrial methods of encapsulation and microencapsulation of high nutritional value oils, imply as a first stage the dispersion of lipid phase in the encapsulating agent aqueous solution (Chan, 2011). During the emulsification process, polymers are organized at oil/water interphase, defining a multiphase solid microstructure when particles are dehydrated (Drusch & Mannino, 2009). Therefore, emulsion features and stability have a major effect on beads properties (Klaypradit & Huang, 2008), thus, the effect of G on the stability of fish oil-alginate emulsions was studied. Figure 2 shows the volume droplet size distribution of emulsions containing 1 % w/v of alginate (A) (Figure 2 A) or 1 % w/v of alginate and 2% of *P. alba* exudate gum (A+G) (Figure 2 B) immediately after preparation and over storage during 24 h at 25 °C.

Figure 2. Volume droplet size distributions curves of fish oil emulsions containing 1 % of alginate (A) and 1% of alginate and 2% of *Prosopis alba* exudate gum (B), obtained after preparation (□) and after storage at 25 °C for 0.5 h (●),1 h (▲), 2 h (✳) and 24 h (◁).
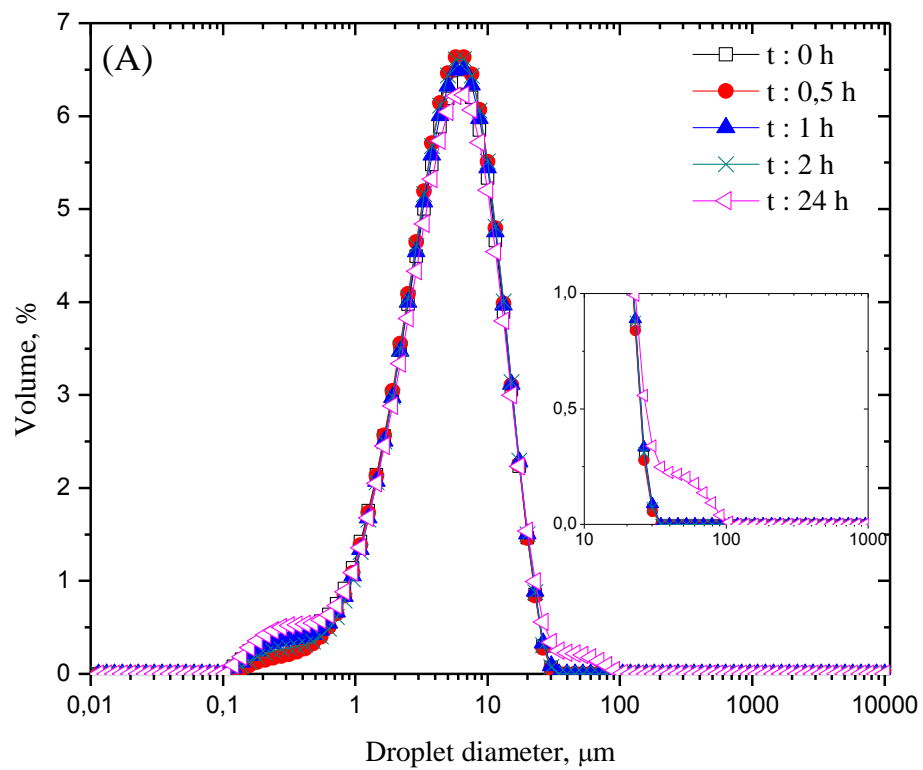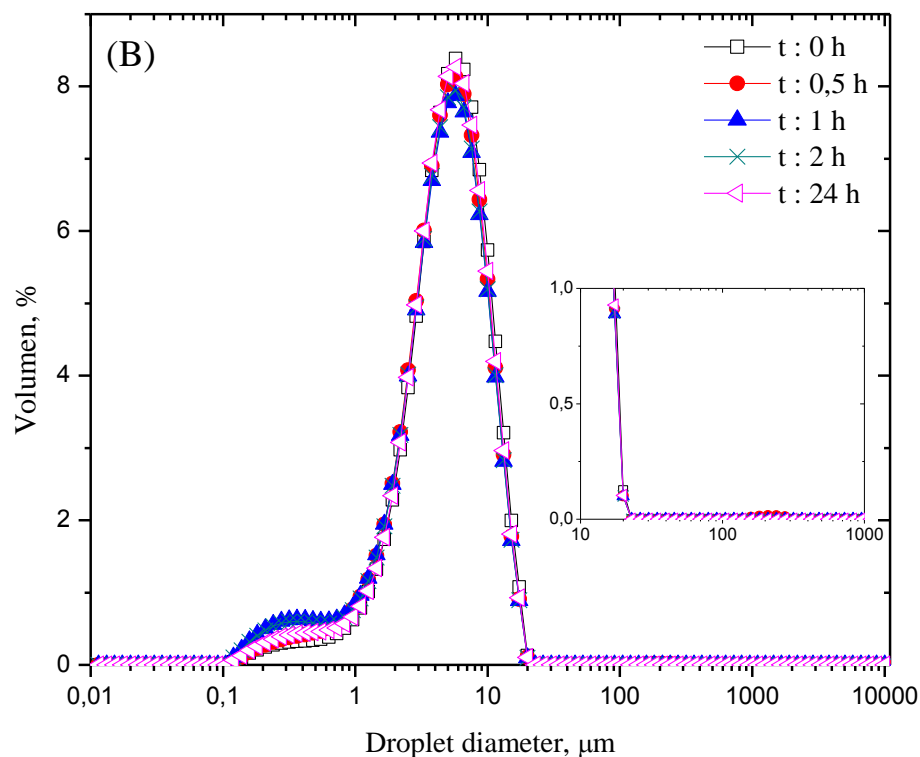
The droplet size distributions of A emulsions after preparation, showed a bimodal distribution with a primary wide peak from 0.1 to 30 µm centered around 7 µm and a secondary peak centered around 0.3 µm. No changes of the distributions were observed over time, except for the last time evaluated (24 h) at which a shoulder from 60 to 100 µm was noticed, indicating the presence of higher droplets size. The droplet size distribution of A+G emulsion immediately after preparation (Figure 2 B) showed a similar emulsifying capacity than A (Figure 2 A), exhibiting a primary wide peak (0.1 - 20 µm) centered around 6 µm and a secondary peak centered around 0.3 µm. No appreciable changes were registered in droplet size distributions of A+G emulsions during storage at 25 °C (Figure 2 B). The mean diameter of most of the droplets, evaluated in terms of $D_{3,2}$ for both emulsions (Table 1) did not show significant differences even after 24 h.

The increase in the droplet size is an indicator of lower polymer emulsification power (Wilde, 2000), therefore G might be useful to improve the ability of A to stabilize a given surface area. As shown in a previous work (Vasile, Martinez, et al., 2016), G decreases the surface tension and forms viscoelastic films at o/w interface, being the good emulsifying properties of G mainly related to its high protein content (13.81 ± 0,33 % db.).

The change in the droplet size of the emulsion was also studied by De Broucker diameter ($D_{4,3}$), which has been widely used for evaluating destabilization processes (Galazka et al., 1996; Relkin & Sourdet, 2005). The $D_{4,3}$ diameters obtained from size distributions, were plotted in Figure 3 for oil emulsions (10%) stabilized with A or A+G. Additionally, the evolution of $D_{4,3}$ diameters of an emulsion containing the oil and 2 % of G was evaluated for comparative purposes.

Figure 3. $D_{4,3}$ diameter calculated from the droplet size distribution of emulsions containing 1 % of alginate (A), 2 % of *Prosopis alba* exudate gum (G) and 1 % of alginate and 2 % of *Prosopis alba* exudate gum (A+G) over time.
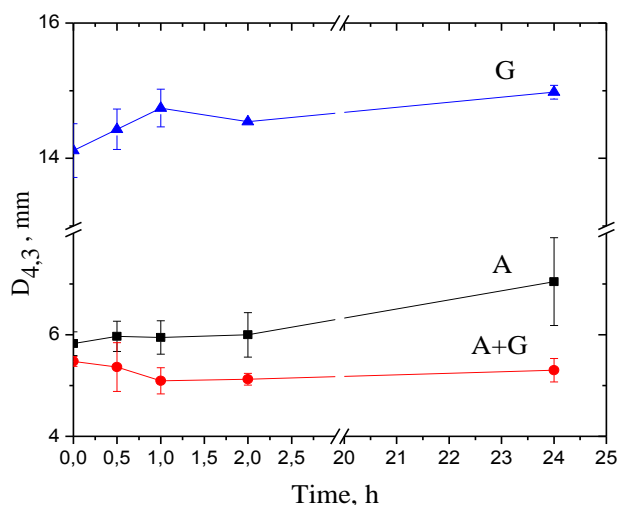
The evolution of $D_{4,3}$ showed significant differences between the systems. Compared with the emulsion stabilized only with G, emulsions containing alginate (A and A+G) promoted the formation of smaller drops during the emulsification process (Figure 3). Being alginate an hydrophilic polysaccharide, it is expected to have a low surface activity (Chan, 2011). Therefore, the reduction in the droplet size in alginate emulsions (Figure 3) could be principally related to an increase viscosity of the continuous phase surrounding the oil droplets that restrict their movement, aggregation and flocculation (Dickinson, 2009, Chan, 2011). $D_{4,3}$ diameter for A+G emulsions (Figure 3) practically remained unchanged after 24 h of storage at 25 °C. In contrast, $D_{4,3}$ values for A and G emulsions tended to increase during storage, being the values higher than the obtained for A+G emulsions even immediately after preparation. $D_{4,3}$ diameter evaluated after 24 h are also shown in Table 1 along with $D_{3,2}$ values. The incorporation of G favors the formation of emulsions with smaller droplets size, which remain stable after 24 h at room temperature, confirming the emulsifying and stabilizing properties of G in the mixture. This time assures the stability of the emulsions during the ionic gelation process. According to the preparation method (Section 2.2.3), the time needed to complete the encapsulation process for a batch of 10 g of the emulsion is less than 30 min.

ζ-potential was also determined for the studied emulsions in order to better understand their stability in terms of polymers interactions. The ζ-potential values for all the emulsions immediately after preparation were below – 30 mV (Table 1), which is usually consider a limit value for achieving significant droplet stabilization by electrostatic repulsion (Guzey & McClements, 2007). The absolute ζ-potential value for G emulsion was lower than emulsion stabilized with A. While, the absolute ζ-potential for the combined (A+G) emulsions was lower than that of A emulsions and it could be interpreted in terms of a partial charges neutralization between positive patches exposed on the protein fraction of G with negatively charged groups present in A. Due to the high protein fraction, G is

expected to have a higher surface activity than A (Dickinson, 2003; Román-Guerrero et al., 2009). According to Dickinson et al. (2011), in composite colloidal systems, emulsions are firstly stabilized by the more surface-active component. In this sense, G probably adsorbed first to the o/w interface providing a net negative charge distribution. Additionally, if associative interactions between positively charged amino acids moieties of G and negatively charged A groups occur, it could lead to a partial adsorption of A on G-coated droplets increasing negative charge distribution compared with G emulsions.

Complementary, no phase separation was observed in A+G emulsions stored at 25 °C, even after 24 h. In contrast, A emulsion exhibited a gel-like microstructure with a separated layer of aqueous serum (opalescent) at the bottom. This phenomena known as depletion by interdroplet pair potential, appears in emulsions where droplets are surrounded by a high concentration of colloidal non-adsorbed molecules which remain in the continuous phase (Fioramonti, Martinez, Pilosof, Rubiolo, & Santiago, 2015). In presence of G, the partial adsorption of A on G-coated droplets, probably reduce the concentration of the polyelectrolytes in the aqueous phase, preventing the interconnected flocks formation. These observations further support the positive effect of G on the stabilization of A emulsion, before encapsulation by ionic gelation.

Table 1. Emulsifying properties of fish oil emulsions stabilized with 1% alginate (A) and 1% alginate + 2% *Prosopis alba* exudate gum (A+G). Emulsion stabilized with 2% gum (G) was also evaluated for comparative purposes. t24: after 24 h of storage at 25 °C.

|	G	A	A + G
$D_{3.2}$*, µm	7.52 ± 0.0[b]	2.36 ± 0.3[a]	2.51 ± 0.2[a]
$D_{3.2}$, µm (t24)	7.2 ± 0.4[b]	2.52 ± 0.1[a]	2.54 ± 0.1[a]
$D_{4..3}$*, µm	14.5 ± 0.0[c]	5.99 ± 0.44[b]	5.12 ± 0.1[a]
$D_{4..3}$, µm (t24)	14.98 ± 0.1[c]	7.05 ± 0.9[b]	5.30 ± 0.2[a]
ζ-potential*, mV	-44.1 ± 0.0[a]	-90.6 ± 0.0[c]	-71.2 ± 0.0[b]

* After preparation (zero time).

Mean ± SD values followed by lowercase letters within the same row are significantly different according to ANOVA at P≤0.05.

3.3. Effect of composition and drying method on oil retention and stability

Porosity of Ca-alginate beads was highlighted as one of the main issues to overcome, especially in holding the active inside structure and preventing the contact of highly oxidizable compounds with oxygen air. Different hydrocolloids matrices and multilayer structures have been proposed in order to modulate the pore size and network complexity for improving the performance of the carrier systems (Bhattarai et al., 2011; Yang, Han, Zheng, Dong, & Liu, 2015). The drying method also affects the structural properties of the beads (Chan, 2011) and hence their retention and protection capacity. In present work, the influence of G as component of the wall material, and chitosan (Ch) as outer shell, were studied, on the physical and structural characteristics of the alginate beads by two drying methods (vacuum and freeze-drying). Previous studies based on physicochemical interactions among polyelectrolytes by FT-IR, reported that G did not affect the interactions between the protonated amino groups of Ch and the dissociated carboxylate groups of A, allowing the effective adsorption of chitosan onto A+G beads (AG-Ch) (Vasile, Romero, et al., 2016).

To evaluate the porosity and possible active/wall material interactions, the oil retention capacity of the beads to successive n-hexane extractions was evaluated as previously described by other authors (Correa, 2003). Figure 4 shows the oil solvent extraction profiles from freeze-dried (Figure 4A) and vacuum-dried (Figure 4B) beads.

Figure 4. Profiles of oil solvent (n-hexane) extraction from freeze-dried and vacuum-dried alginate beads. Ca-alginate (A), Ca-alginate-chitosan (A-Ch), Ca-alginate-gum (AG), and Ca-alginate-gum-chitosan (AG-Ch) beads.
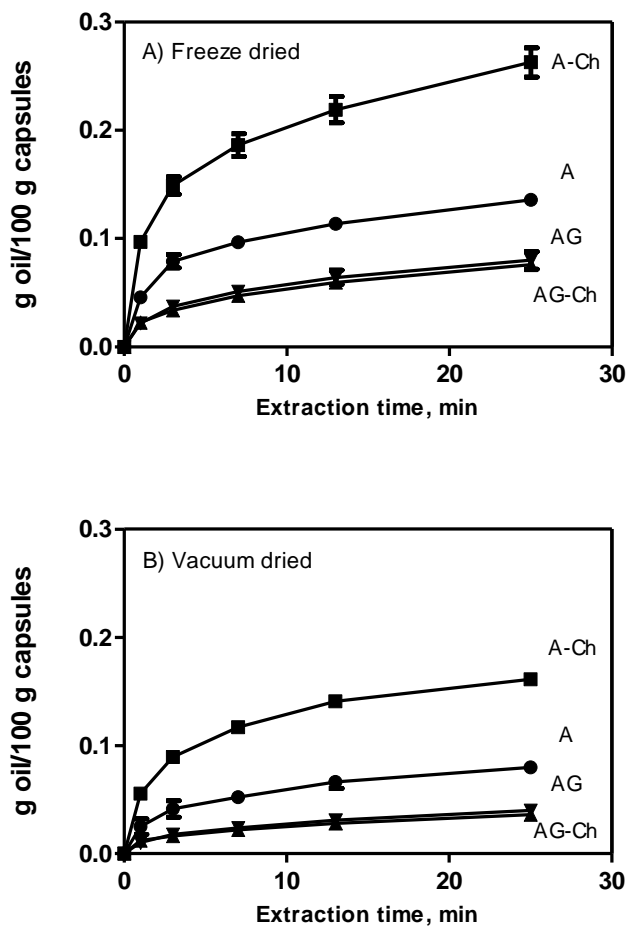
Both the beads composition and the drying method affected the oil retention capacity of polyelectrolytes beads. In all cases, the extractable oil (expressed as g of oil/100 g of capsules), was found to follow a similar trend with a sharp increasing at the beginning of extraction before leveling off. The oil diffusion from inside the beads to the surface, could be related to different structural characteristics according to reported by other authors (Chan, 2011; Puguan, Yu, & Kim, 2014).

Regardless of composition, vacuum-dried beads retained better the oil (0.02 to 0.17 g extracted oil / 100 g beads) than the freeze-dried ones (0.06 to 0.3 g extracted oil / 100 g

capsules), as is shown in Figure 4 B and A, respectively. Similar results were related by Chan et al. (2011) with the porous internal structure resulting from water crystals sublimation during freeze-drying. This macroporous structure favors the oxygen diffusion and hence reduce the retention and stability of the oil. Rapid water surface evaporation and solutes displacement during vacuum-drying, lead to a more compact shell hindering the solvent penetration and oil extraction (Smrdel, Bogataj, & Mrhar, 2008).

Chitosan coating was proposed as an approach to increase the density and crosslinking of polymers at surface of alginate beads in order to limit the active diffusion (Garti & McClements, 2012; Peniche et al., 2004). However, in present work the beads coated with chitosan retained less oil against solvent extraction compared to no coated systems, independently of the drying method. The presence of G improved the retention of the oil inside the alginate beads even in the absence of chitosan. However, no negative effect of chitosan was observed and a chitosan coating could be beneficial considering its antimicrobial, biodegradability and mucoadhesive properties (Arancibia et al., 2015; Çetinus, Şahin, & Saraydin, 2009; Ma, Zhang, & Zhong, 2016). The extractable oil at equilibrium (g oil/ 100 g of beads) for vacuum and freeze dried chitosan coated beads was estimated by fitting the experimental data (Figure 4) to a two-phase decay model, the obtained values are summarized in Table 2. The positive effect of G on the oil retention capacity could be related with gum composition and molecular polymer interactions in the solid matrix. The presence of low molecular weight sugars in G could act filling the void spaces in the polymeric network favoring the formation of a more compact matrix. According to Drusch (2009), low molecular weight carbohydrates also reduce the oxygen permeability increasing the core material stability. Pongjanyakul et al. (2007) state that the addition of gums to the alginate matrix increase the tortuosity of encapsulating material limiting the diffusion of the active. Thus, G could also establish intermolecular hydrogen bonds with other polyelectrolytes in the bead matrix increasing the tortuosity and hindering

the oil extraction. Besides, the best emulsifying properties of A+G composite blends probably contribute to the higher retention, providing a physical barrier at the o/w interface that hinders the oil diffusion.

In order to evaluate the stability of the encapsulated oil in accelerated thermal conditions, DSC oxidative assays were performed on vacuum and freeze-dried chitosan-coated beads. The temperature at which a change in slope was observed in the curve of heat flow versus temperature, was related with the final oxidation stages (Shahidi & Zhong, 2005). Table 2 shows the onset temperature of oxidation for the studied systems.

Independently of the drying method, oxidation of the encapsulated oil occurred at higher temperatures (166 - 187°C) in comparison with the free oil (157 ± 1 °C). Structural features of encapsulates could partly explain the different oxidative stabilities (Drusch & Mannino, 2009).

The oxidation temperatures determined for vacuum-dried beads were higher than those measured for the freeze-dried systems (Table 2), indicating that the freeze-dried structure negatively affected the core protection. This result agreed with the structural features observed in the accelerated solvent extraction assay (Figure 4).

Considering the composition, freeze-dried beads did not show significant differences on the oxidation onset temperature. However, in vacuum-dried systems containing G as component of the wall material, oxidation occurred at a higher temperature (187 ± 1 °C). G could act improving the structural features of encapsulates as well as providing compounds with antioxidant activity (Vasile, Romero, et al., 2016). Polyphenols, tannins and reducing sugars naturally present in G could contribute to the oil stabilization. Similarly, Pérez-Alonso et al. (2008) found that mesquite gum addition to whey-maltodextrin matrixes increased the thermal oxidation temperature of chili oleoresin microparticles obtained by spray drying.

In freeze-dried AG-Ch beads, the structural features of encapsulates governed the susceptibility to lipid oxidation and the benefits of the gum were not evident. From these results, vacuum drying method was chosen as adequate in order to improve the fish oil protection

3.4. Structural and morphological characterization of the dried beads containing oil

The effect of G as component of the alginate capsule was assessed in terms of oil distribution, encapsulation efficiency and yield of the encapsulation process, and also by evaluating the external morphology, internal microstructure and size distribution. Table 2 shows the oil distribution determined for the vacuum-dried A-Ch and AG-Ch beads.

Despite the higher solid/oil ratio of the AG-Ch emulsion respect to A-Ch, the total oil content (TO) was not significantly different in the dried beads. AG-Ch presented a higher internal oil fraction (IO), and a lower surface oil fraction (SO) compared to A-Ch. Accordingly, AG-Ch beads were perceived less oily and sticky than A-Ch during handling.

Oil beads distribution has different stability and technological implications. It's known that a higher surface oil fraction increases the susceptibility to oxidation of the capsules (Velasco, Holgado, Dobarganes, & Márquez-Ruiz, 2009) and also makes them difficult to handle, fractionate and transport. On the other hand, a good oil load capacity is generally sought when a low volume of encapsulates is required for a specific application (Chan, 2011). In this sense, the incorporation of *P. alba* gum allowed to obtain beads with lower SO and higher IO percentage than A-Ch. The effect of G was clearly reflected in a higher encapsulation efficiency (EE) (Table 2). The highest EE in dehydrated bead systems containing G could be explained considering its contribution on structural features.

31

Changes in the emulsion properties in the presence of the gum (Table 1) could probably affect the oil distribution in beads. It was observed that a stable emulsion with minimum droplet size, reduced the non-encapsulated oil at the surface of particles (Chan, 2011). Additionally, other authors observed that a stabilized emulsion prevents the diffusion of oil drops to the surface during the gel crust formation, increasing the encapsulation efficiency (Aghbashlo, Mobli, Madadlou, & Rafiee, 2012) and reducing the active losses during beads generation. Hence, the barrier properties at oil/water interface could improve the oil retention capacity in the hydrogel matrix. Additionally, after beads generation, vacuum drying increase the oil surface fraction. This was previously described by Chan et al. (2011), who attributed the oil outflow at beads surface to the gel shrinkage during drying. These facts allow to consider that G could act reducing the gel contraction thereby increasing the oil retention in the internal structure of the dehydrated beads.

The encapsulation yield also showed the benefits of incorporating the gum as wall material (Table 2). The encapsulation yield (EY), expressed as the percentage of total oil relative to the oil weighted in the emulsion, indirectly quantifies the oil losses through the overall encapsulation process. Chan (2011) state that oil losses could be mainly explained considering a deficient entrapment during gelation process. In this regard, G probably promote the formation of a tight Ca-alginate-gum hydrogel barrier improving the gelling density by supply of endogenous Ca^{2+} ions, or well due to specific A+G interactions, as was previously described in ternary phase diagram (Figure 1B). (Pongjanyakul & Puttipipatkhachorn, 2007) also found a better entrapment capacity of gel alginate beads when xanthan gum was added as excipient.

The size distribution of dried A-Ch and AG-Ch beads was determined by digital image analysis. Figure 5 shows the frequency distribution of diameters for A-Ch (Figure 5A) and AG-Ch (Figure 5B) beads.

Figure 5. Frequency size distribution (diameter, mm) of alginate-chitosan (A) and alginate-gum-chitosan (B) capsules obtained by digital image analysis.
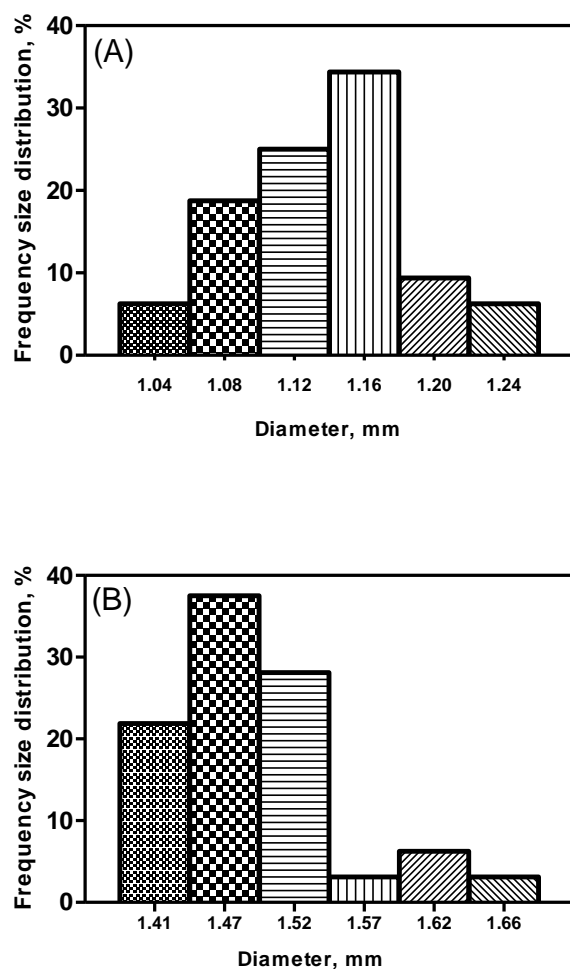
In absence of the gum (Figure 5A), A-Ch capsules showed a monomodal and symmetric size distribution centered at 1.16 mm, while for AG-Ch capsules (Figure 5B) an asymmetric monomodal distribution, centered at 1.47 mm was observed. The introduction of the gum increased significantly the mean diameter of beads (Table 2). Similarly, Pongjanyakul et al. (2007), observed higher bead mean diameters when xanthan gum was used as excipient in alginate beads. Wang et al. (2013) also found a size increasing for Ca-alginate beads containing canola oil and pectin as excipient.

33

The higher size of AG-Ch could partially explain the lower SO fraction considering that higher size particles present a lower surface area for oil loss. Additionally, less exposed surface area could leads to a lower oxidation rate (Augustin, Sanguansri, Decker, Elias, & McClements, 2010), as well as to a delay favorably the encapsulated lipids digestibility in the gastrointestinal tract (Li, Hu, Du, Xiao, & McClements, 2011). However, large capsules are more easily perceived in the food which may be desirable for certain products, but undesirable for others (Gaonkar, Vasisht, Khare, & Sobel, 2014; Oxley, 2012).

Table 2. Structural and stability properties of freeze-dried and vacuum-dried polyelectrolytes beads containing fish oil. Alginate-chitosan beads (A-Ch). Alginate-*Prosopis alba* exudate gum-chitosan beads (AG-Ch). TO: Total oil; IO: internal oil; SO: Surface Oil; EE: encapsulation efficiency; EY: encapsulation yield.
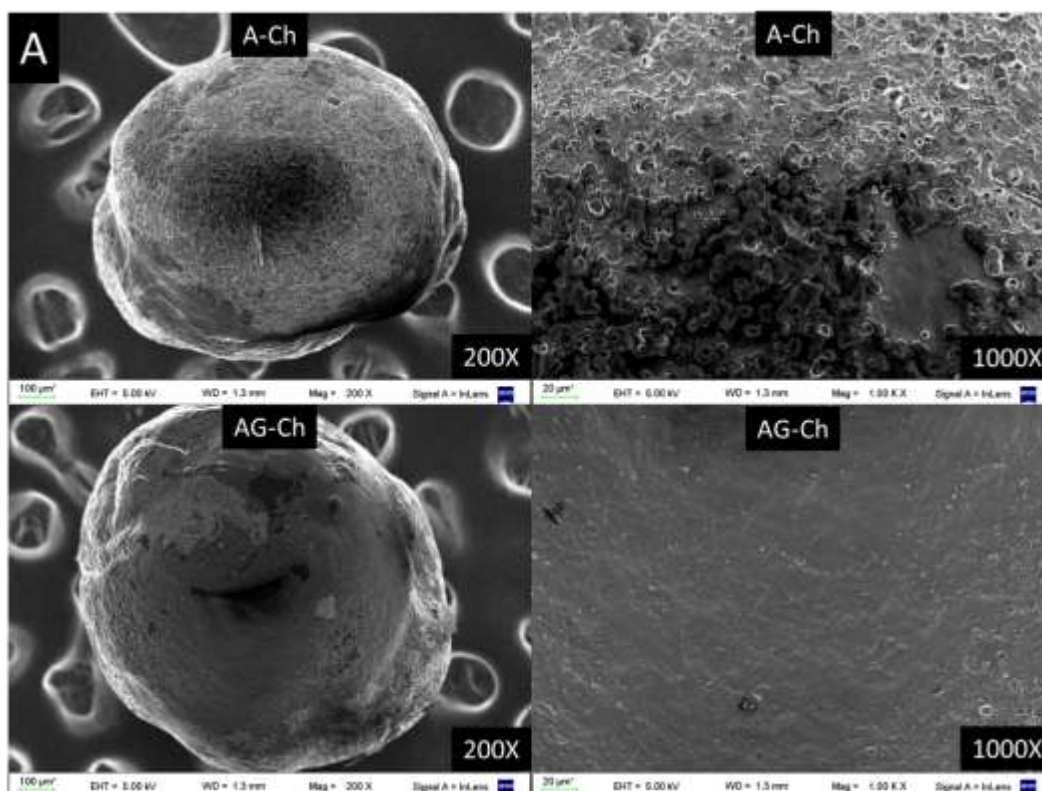
	Vacuum dried beads		Freeze dried beads	
	A-Ch	AG-Ch	A-Ch	AG-Ch
Extractable oil (g oil / 100 g beads)	0.17 ± 0.0	0.05 ± 0.0	0.3 ± 0.1	0.09 ± 0.0
Onset oxidation temperature, °C	174 ± 1^b	187 ± 1^c	168 ± 2^a	166 ± 2^a
TO, % db.	78.29 ± 0.0^a	77.97 ± 1.7^a	ND	ND
IO, % db.	70.43 ± 0.4^a	76.90 ± 1.7^b	ND	ND
SO, % db.	7.87 ± 0.5^b	1.07 ± 0.0^a	ND	ND
EE, %	89.95 ± 0.6^a	98.63 ± 0.0^b	ND	ND
EY, %	70.72 ± 0.2^a	89.12 ± 0.1^b	ND	ND
Mean diameter, mm	1.14 ± 0.0^a	1.49 ± 0.1^b	ND	ND

Mean ± SD values followed by lowercase letters within the same column, or capital letters within the same row are significantly different according to two way ANOVA test at P≤0.05.

The effect of the composition was also studied on the structural characteristics of the encapsulated using scanning electron microscopy (SEM). Figure 5 shows the external

morphology (Figure 6A) and the internal structure (Figure 6B) of vacuum dried A-Ch and

AG-Ch beads.

Figure 6. Micrographs of external morphology (A) and internal structure (B) of vacuum dehydrated alginate-chitosan (A-Ch) or alginate-gum-chitosan (AG-Ch) beads.
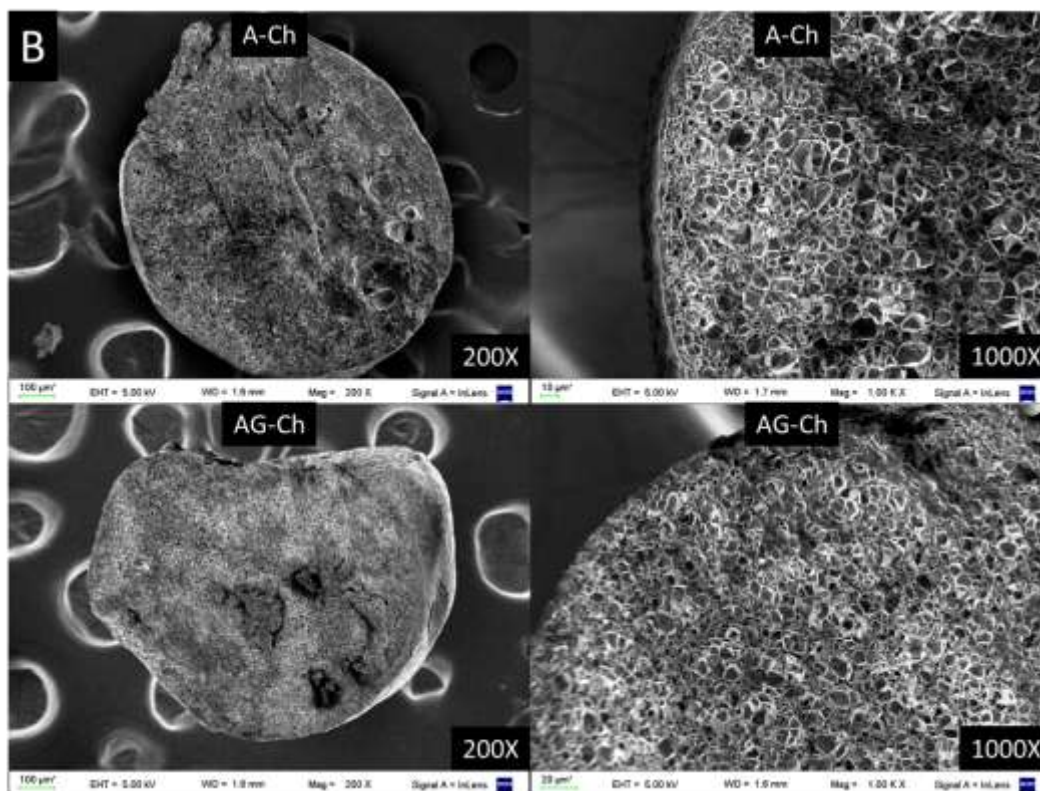
Figure 6 shows that vacuum dried beads presented a rather spherical shape independently of the composition. The beads containing the gum were larger and had a smoother surface than A-Ch, evidencing a continuous and denser structure. The more compact surface of AG-Ch was related to the presence of low molecular weight sugars naturally present in the gum, which could act filling voids in the polymer network. The smooth and continuous surface, without cracks or holes, seems to favors the retention of the active compound within the carrier matrix. These observations are in agreement with the better oil retention capacity determined for AG-Ch (Figure 4), and their higher oxidative stability (Table 2). The vacuum-dried A-Ch beads had an irregular surface, with hollows and more roughness, as well as traces of oil in the surface.

The cross-sectional images showed that all both systems have an internal structure of "multicore" type, resulting from the gelation process of the emulsion. In presence of G, cavities were smaller and uniformly distributed. These characteristics could be related with

the lower droplet size distribution and higher emulsion stability of A+G emulsions prior to gelation process.

4. Conclusions

In present work, the encapsulation of fish oil in Ca-alginate beads using a novel exudate gum *Prosopis alba* as excipient was studied. Sol-gel phase diagrams were made to study the polyelectrolyte interactions and its effect on physical state of the aqueous suspension. Phase diagrams proved to be a useful and easy tool to select adequate physical behavior of alginate-gum blends for oil emulsification and for later gelification. They allowed to define the most suitable polyelectrolyte concentration (G and alginate) and of the crosslinker agent ($CaCl_2$) for preparing capsules by external ionic gelation, as well as the effect of G in the combined matrix. The system containing 1% w/v alginate and 2% w/v of G leads to suspensions with good flow characteristics, suitable for later emulsion and dripping stages. Furthermore, it was determined that solutions of $CaCl_2$ 2% w/v were sufficient to induce instantaneous gelation, with high water holding capacity, and hence efficient entrapment of the active. Combined alginate-gum suspensions were suitable both for oil emulsification and beads generation. The studied gum improved the emulsion properties (lower droplet size distribution and higher stability) and hence the oil encapsulation efficiency and yield after vacuum drying. In dehydrated beads, G modulated the matrix structure, improving oil retention and stability in accelerated thermos-oxidative assays. Present results are promising and allowed considering *P. alba* gum as a novel non-conventional polyelectrolyte for improving Ca-alginate beads microstructure and stability with the added benefit of taking advantage of an available resource currently untapped.

5. Bibliography

Abang, S., Chan, E.-S., & Poncelet, D. (2012). Effects of process variables on the encapsulation of oil in ca-alginate capsules using an inverse gelation technique. *Journal of Microencapsulation,* 29(5), 417-428.

Aghbashlo, M., Mobli, H., Madadlou, A., & Rafiee, S. (2012). The correlation of wall material composition with flow characteristics and encapsulation behavior of fish oil emulsion. *Food Research International,* 49(1), 379-388.

Arancibia, M. Y., López-Caballero, M. E., Gómez-Guillén, M. C., Fernández-García, M., Fernández-Martín, F., & Montero, P. (2015). Antimicrobial and rheological properties of chitosan as affected by extracting conditions and humidity exposure. *LWT - Food Science and Technology,* 60(2, Part 1), 802-810.

Augustin, M., Sanguansri, L., Decker, E., Elias, R., & McClements, D. (2010). Use of encapsulation to inhibit oxidation of lipid ingredients in foods. *Oxidation in foods and beverages and antioxidant applications. Volume 2: Management in different industry sectors*, 479-495.

BeMiller, J. N., & Huber, K. C. (2007). *Chapter 3: Carbohydrates.* In *Fenema´s Food Chemistry Fourth Edition* (pp. 83 - 154)

Bhattarai, R. S., Dhandapani, N. V., & Shrestha, A. (2011). Drug delivery using alginate and chitosan beads: An Overview. *Chronicles of Young Scientists,* 2(4), 192.

Çetinus, Ş. A., Şahin, E., & Saraydin, D. (2009). Preparation of Cu (II) adsorbed chitosan beads for catalase immobilization. *Food Chem,* 114(3), 962-969.

Córdoba, A. L., Deladino, L., & Martino, M. (2013). Effect of starch filler on calcium-alginate hydrogels loaded with yerba mate antioxidants. *Carbohydrate Polymers,* 95(1), 315-323.

Correa, R. M. (2003). Preparo e caracterização de microcapsulas obtidas por polimerização ionica para alimentação de larvas de peixe. Universidade Estadual de Campinas (UNICAMP). Faculdade de Engenharia de Alimentos.

Chan, E.-S. (2011). Preparation of Ca-alginate beads containing high oil content: Influence of process variables on encapsulation efficiency and bead properties. *Carbohydrate Polymers,* 84(4), 1267-1275.

Deladino, L., Anbinder, P. S., Navarro, A. S., & Martino, M. N. (2008). Encapsulation of natural antioxidants extracted from Ilex paraguariensis. *Carbohydrate Polymers,* 71(1), 126-134.

Dickinson, E. (2003). Hydrocolloids at interfaces and the influence on the properties of dispersed systems. *Food Hydrocolloids,* 17(1), 25-39.

Dickinson, E. (2011). Mixed biopolymers at interfaces: Competitive adsorption and multilayer structures. *Food Hydrocolloids,* 25(8), 1966-1983.

Drusch, S., & Mannino, S. (2009). Patent-based review on industrial approaches for the microencapsulation of oils rich in polyunsaturated fatty acids. *Trends in Food Science & Technology,* 20(6–7), 237-244.

Fioramonti, S. A., Martinez, M. J., Pilosof, A. M., Rubiolo, A. C., & Santiago, L. G. (2015). Multilayer emulsions as a strategy for linseed oil microencapsulation: effect of pH and alginate concentration. *Food Hydrocolloids,* 43, 8-17.

Galazka, V. B., Dickinson, E., & Ledward, D. A. (1996). Effect of high pressure on the emulsifying behaviour of β-lactoglobulin. *Food Hydrocolloids,* 10(2), 213-219.

Garti, N., & McClements, D. J. (2012). *Encapsulation technologies and delivery systems for food ingredients and nutraceuticals*: Elsevier.

Grant, G. T., Morris, E. R., Rees, D. A., Smith, P. J., & Thom, D. (1973). Biological interactions between polysaccharides and divalent cations: the egg-box model. *FEBS letters,* 32(1), 195-198.

Guzey, D., & McClements, D. J. (2007). Impact of Electrostatic Interactions on Formation and Stability of Emulsions Containing Oil Droplets Coated by β-Lactoglobulin−Pectin Complexes. *Journal of Agricultural and Food Chemistry,* 55(2), 475-485.

Hunter, R. J. (2001). *Foundations of colloid science / Robert J. Hunter*. Oxford ; New York: Oxford University Press.

Klaypradit, W., & Huang, Y.-W. (2008). Fish oil encapsulation with chitosan using ultrasonic atomizer. *LWT-Food Science and Technology,* 41(6), 1133-1139.

Lee, K. Y., & Mooney, D. J. (2012). Alginate: properties and biomedical applications. *Progress in polymer science,* 37(1), 106-126.

Leroux, J., Langendorff, V., Schick, G., Vaishnav, V., & Mazoyer, J. (2003). Emulsion stabilizing properties of pectin. *Food Hydrocolloids,* 17(4), 455-462.

Li, Y., Hu, M., Du, Y., Xiao, H., & McClements, D. J. (2011). Control of lipase digestibility of emulsified lipids by encapsulation within calcium alginate beads. *Food Hydrocolloids,* 25(1), 122-130.

Ma, Q., Zhang, Y., & Zhong, Q. (2016). Physical and antimicrobial properties of chitosan films incorporated with lauric arginate, cinnamon oil, and ethylenediaminetetraacetate. *LWT - Food Science and Technology,* 65, 173-179.

Mestdagh, M., & Axelos, M. (1999). Physico-chemical properties of polycarboxylate gel phase and their incidence on the retention/release of solutes. *Les Colloques de l'INRA*, 303-314.

Pawar, S. N., & Edgar, K. J. (2012). Alginate derivatization: A review of chemistry, properties and applications. *Biomaterials, 33*(11), 3279-3305.

Peniche, C., Howland, I., Carrillo, O., Zaldívar, C., & Argüelles-Monal, W. (2004). Formation and stability of shark liver oil loaded chitosan/calcium alginate capsules. *Food Hydrocolloids, 18*(5), 865-871.

Pérez-Alonso, C., Cruz-Olivares, J., Barrera-Pichardo, J., Rodríguez-Huezo, M., Báez-González, J., & Vernon-Carter, E. (2008). DSC thermo-oxidative stability of red chili oleoresin microencapsulated in blended biopolymers matrices. *Journal of Food Engineering, 85*(4), 613-624.

Pongjanyakul, T., & Puttipipatkhachorn, S. (2007). Xanthan–alginate composite gel beads: Molecular interaction and in vitro characterization. *International Journal of Pharmaceutics, 331*(1), 61-71.

Puguan, J. M. C., Yu, X., & Kim, H. (2014). Characterization of structure, physico-chemical properties and diffusion behavior of Ca-Alginate gel beads prepared by different gelation methods. *Journal of Colloid and Interface Science, 432*, 109-116.

Rehm, B. H. A. (2009). *Alginates: Biology and Applications: Biology and Applications*: Springer.

Relkin, P., & Sourdet, S. (2005). Factors affecting fat droplet aggregation in whipped frozen protein-stabilized emulsions. *Food Hydrocolloids, 19*(3), 503-511.

Román-Guerrero, A., Orozco-Villafuerte, J., Pérez-Orozco, J. P., Cruz-Sosa, F., Jiménez-Alvarado, R., & Vernon-Carter, E. J. (2009). Application and evaluation of mesquite gum and its fractions as interfacial film formers and emulsifiers of orange peel-oil. *Food Hydrocolloids, 23*(3), 708-713.

Shahidi, F., & Zhong, Y. (2005). Lipid oxidation: measurement methods. *Bailey's industrial oil and fat products*.

Smrdel, P., Bogataj, M., & Mrhar, A. (2008). The influence of selected parameters on the size and shape of alginate beads prepared by ionotropic gelation. *Scientia Pharmaceutica,* 76(1), 77.

Sun-Waterhouse, D., Zhou, J., Miskelly, G. M., Wibisono, R., & Wadhwa, S. S. (2011). Stability of encapsulated olive oil in the presence of caffeic acid. *Food Chem,* 126(3), 1049-1056.

Vasile, F. E., Martinez, M. J., Ruiz-Henestrosa, V. M. P., Judis, M. A., & Mazzobre, M. F. (2016). Physicochemical, interfacial and emulsifying properties of a non-conventional exudate gum (Prosopis alba) in comparison with gum arabic. *Food Hydrocolloids,* 56, 245-253.

Vasile, F. E., Romero, A. M., Judis, M. A., & Mazzobre, M. F. (2016). Prosopis alba exudate gum as excipient for improving fish oil stability in alginate–chitosan beads. *Food Chem,* 190, 1093-1101.

Velasco, J., Holgado, F., Dobarganes, C., & Márquez-Ruiz, G. (2009). Influence of relative humidity on oxidation of the free and encapsulated oil fractions in freeze-dried microencapsulated oils. *Food Research International,* 42(10), 1492-1500.

Wang, W., Waterhouse, G. I. N., & Sun-Waterhouse, D. (2013). Co-extrusion encapsulation of canola oil with alginate: Effect of quercetin addition to oil core and pectin addition to alginate shell on oil stability. *Food Research International,* 54(1), 837-851.

Wichchukit, S., Oztop, M., McCarthy, M., & McCarthy, K. (2013). Whey protein/alginate beads as carriers of a bioactive component. *Food Hydrocolloids,* 33(1), 66-73.

Wilde, P. J. (2000). Interfaces: their role in foam and emulsion behaviour. *Current Opinion in Colloid & Interface Science,* 5(3–4), 176-181.

Yang, J., Han, S., Zheng, H., Dong, H., & Liu, J. (2015). Preparation and application of micro/nanoparticles based on natural polysaccharides. *Carbohydrate Polymers, 123*, 53-66.